Journal of the European Ceramic Society 21 (2001) 119–126

www.elsevier.com/locate/jeurceramsoc

Innovative methods for preparation and testing of Al_2O_3 supported silicalite-1 membranes

G.E. Romanos [a], Th.A. Steriotis [a,*], E.S. Kikkinides [a], N.K. Kanellopoulos [a], V. Kasselouri [b], J.D.F. Ramsay [c], P. Langlois [c], S. Kallus [c]

[a] *NCSR DEMOKRITOS, Institute of Physical Chemistry, 15310 Ag. Paraskevi Attikis, Greece*
[b] *NTU of Athens, Chem. Eng. Dept, Iroon Polytechniou 7, Zografou, Athens, Greece*
[c] *Laboratoire des Matériaux et Procédés Membranaires, UMR CNRS 5635, Université Montpellier II, Montpellier, France*

Received 15 January 2000; received in revised form 31 May 2000; accepted 11 June 2000

Abstract

The aim of the present study is to develop a novel type of zeolite membrane and exploit some of the inherent and unique advantages of this membrane in gas separations. The development of inorganic membranes formed from a coherently grown layer of zeolite crystals is a particularly promising approach, since such membranes offer substantially higher permeabilities and selectivities compared with polymeric materials and can perform under extreme conditions, e.g. at elevated temperatures and in aggressive chemical environment. Such zeolite membranes are prepared by in-situ hydrothermal synthesis of zeolite layer within the macropores of alumina ceramic supports (tubes/discs). In this way more stable zeolite membranes are produced, avoiding outer separating layers which are prone to mechanical damage. These membranes have also been shown to have good thermal stability up to 500°C, with no evidence of crack formation. The synthesized materials have been characterized by several techniques such as Hg and N_2 porosimetry, scanning electron microscopy (SEM), and X-ray diffraction (XRD). From these measurements it appears that the structure of the zeolite membrane is influenced by several factors, such as structure and size of the pores of the support, chemical composition of the precursor solution from which the crystals will be harvested, reaction conditions, etc. Finally, gas permeabilities and/or selectivities have been measured for several important gas systems. The results of this study indicate the important role of influencing the outcome of the crystal formation by controlling the conditions of the hydrothermal treatment in obtaining optimum gas permeabilities and/or selectivities of these systems.

Keywords: Al_2O_3; Hydrothermal methods; Membranes; Selectivity; Zeolites

1. Introduction

Inorganic membranes have considerable potential for many technical applications because they are characterised by high stability at elevated temperatures combined with chemical resistance even in a corrosive environment.[1–3] More recently a new research field concerned with ceramic membranes incorporating zeolites has developed rapidly.[4,5] Zeolites are crystalline metal oxides containing micropores. The surfaces that are active in sorptive and catalytic applications are internal and intrinsic to the crystal structure and for this reason these materials have unique properties such as singular pore diameter, well-defined surface properties and high thermal stability, which have made them invaluable in many technical applications.[6,7] By controlling the zeolite synthesis conditions it is possible to grow zeolites as films or layers[8,9] instead of powdered particles. Such a synthesis, using macro-porous ceramic supports, provides a possible route to zeolite membranes. Previous developments, in this field have been predominantly focused on ZSM-5[10] and silicalite-1[11] membranes. Important results concerning the gas permeability and selectivity of silicalite-1 supported on a metallic substrate have been reported recently by Moulijn et al.[12–15] The work here is focused on the in situ growth of zeolite membranes on porous ceramic supports, and has the objective to investigate the influence of the support structure and hydrothermal conditions on the properties of silicalite-1 membranes, synthesised

* Corresponding author. Tel.: +30-1-650-3973; fax: +30-1-651-1766.
E-mail address: tster@mail.demotiritos.gr (Th.A. Steriotis).

0955-2219/01/$ - see front matter
PII: S0955-2219(00)00176-X

using a procedure, which we have developed previously.[5]

2. Experimental

2.1. Membrane synthesis

The macroporous α-alumina supports, in disc or tubular shaped form, were produced commercially (Velterop BV, Netherlands). The discs (25 mm in diameter and 2 mm in thickness) were available with different macropore sizes (0.08, 0.15, 2 and 9 μm). The tubes with an outer diameter of 14 mm and a wall thickness of 3 mm were manufactured with pore size of 2.5 and 9 μm. The macropore structure of these different types of supports was analysed by mercury porosimetry. Changes in the porosity, which occurred after the hydrothermal treatment, were also monitored.

The synthesis solution for silicalite-1 was obtained by dissolving pyrogenic silica (SiO_2, Aerosil 380, Degussa) in an aqueous solution of tetrapropylammonium hydroxide (TPAOH) (Aldrich) as templating agent to give a molar composition of 1 SiO_2:1 TPAOH:56 H_2O. This mixture was aged for 4 days at room temperature to give a clear homogeneous solution of oligomeric silica species. Syntheses were carried out by heating the mixture with the support in 50 ml Teflon lined stainless steel autoclaves at different temperatures (in a range between 130 and 190°C) and various times (from a few days to several weeks). After crystallisation of zeolite the membranes were rinsed with distilled water, dried and further characterised. Before gas permeation experiments, the organic template was removed by calcination up to 500°C under controlled conditions to avoid the formation of defects in the membrane.

2.2. Characterization techniques

The synthesized membranes were characterized through a series of advanced techniques to get information about the film formation and the membrane pore structure after the zeolite growth. These techniques included scanning electron microscopy (SEM), X-ray diffraction (XRD), Hg and N_2 porosimetry.

Apart from characterizing the developed membranes, a series of permeation studies were conducted using several probe molecules such as SF_6, He, N_2, CO_2, CH_4, C_2H_6, C_3H_8, O_2, etc., at different temperatures. The measurements included integral single component low-pressure permeability, differential high-pressure permeability and counter current permeation. Finally, the selectivity of a gas mixture of *n*-hexane (HEX)/2,2 dimethylbutane (DMB) was measured in order to determine the membrane's ability to separate linear from branched paraffins.

All experiments were performed either on a home-made high-pressure rig, described elsewhere[16] or on a Wicke–Kallenbach apparatus. This apparatus is all stainless steel and can perform counter-current experiments (with or without pressure difference) up to 100 bar. The pressure at each side of the membrane can be set from 1 to 100 bar using back pressure regulators and monitored by absolute pressure transducers (Cerabar, 0–100 bar). Small pressure differences between feed and permeate can also be monitored by a differential pressure transducer (Applied Measurements, 0–1000 mbar). The flow of the feed and carrier are controlled via three Brooks 5850 E series mass flow controllers. By appropriate valve arrangement the setup can be reversed so that the feed is introduced either to the macroporous support or the zeolite side. During these experiments both streams are analyzed before and after steady state by means of a Hewlett Packard 5890 Series II Gas Chromatograph, equipped with a ten port, programmable, automatic, gas-sampling valve. For all the experiments the GC carrier gas was Argon and an isothermal method (100°C) was used. Detection was achieved by a thermal conductivity and a flame ionisation detector, connected to Haysep II 80/100 mesh and capillary PLOT Q columns, respectively. Both detectors were pre-calibrated for the gases and vapors used, so that the molar fraction (x) and hence the permeance of each component, along with the counter diffusion of sweep gas could be calculated. Especially for the HEX/DMB selectivity measurements two bubblers (the first filled with *n*-hexane and the second with 2,2 dimethylbutane) were attached after the two mass flow controllers. The composition of the feed stream was controlled by tuning the temperature of the oil baths, were the bubblers containing the liquids were kept, by means of two Julabo EO7 PID temperature controllers. The mixture was fed past the zeolite side of the membrane, using nitrogen as carrier, while helium was used as sweep-gas on the permeate side. The flow was set to around 10 ml/min. The selectivity, S, was then calculated with the equation:

$$S = \frac{x_{\mathrm{HEX}}^{\mathrm{permeate}} / x_{\mathrm{HEX}}^{\mathrm{feed}}}{x_{\mathrm{DMB}}^{\mathrm{permeate}} / x_{\mathrm{DMB}}^{\mathrm{feed}}}$$

where $x_{\mathrm{A}}^{\mathrm{a}}$ is the molar fraction of component (A) on the (a) side of the membrane.

3. Results and discussion

3.1. Zeolite formation

X-ray diffraction is primarily used to ensure crystallinity of the sample and to identify crystal structures. In

Fig. 1(a) and (b) two XRD patterns are shown in comparison, one for the zeolite membrane along with one for the alumina substrate. The sample of pure alumina substrate has a higher degree of crystallinity and fewer peaks while after the zeolite formation the pattern reveals lower crystallinity probably due to the formation of disordered zeolite phase in the pores of the substrate. In addition new peaks appear compared to the case of pure alumina substrate and these are characteristic of the formed silicalite crystals.

3.2. Substrate selection

Experiments were undertaken to optimise the conditions for the formation of defect free silicalite-1 membranes. In the first set of experiments the influence of the ceramic support on the growth of the zeolite film was studied by SEM and mercury porosimetry. Syntheses were performed with the different porous ceramic supports using fixed temperature/time conditions. The crystallinity of the zeolite layer was confirmed by XRD. When the synthesis temperature was kept for 6 days at 190°C, for all the different porous alumina supports, extensive growth of a silicalite-1 layer on the support surface occurred. This is illustrated by the micrographs in Fig. 2(a) and (b), showing a cross-section through two membranes with a substrate of 0.08 and 9 μm. These layers include a dense region near the substrate and a rugged structure on the top, which is formed by individual crystals growing out of the dense phase. In addition to the layer formation on the surface of the ceramic, there is evidence of penetration and pore filling inside the support. The thickness of the outer layer varied between 30 and 80 μm.

The most homogeneous layer was obtained in the case of the ceramic support with the smallest pores (diameter ~0.08 μm) as presented in Fig. 2(a). The surface layer on the 9 μm tubular support had a thicker rugged region and thinner dense region, the boundary between the layer and the support being ill defined [Fig. 2(b)]. Synthesis conditions, which either favoured the growth of a well-crystallised zeolite layer on the surface of the ceramic support or the preferential formation of a zeolite phase within the macropores of the alumina sublayer, were further studied. In order to increase the penetration frontier inside the pores of the support and to minimise extensive surface growth of zeolite, kinetic investigations at lower temperatures were carried out.

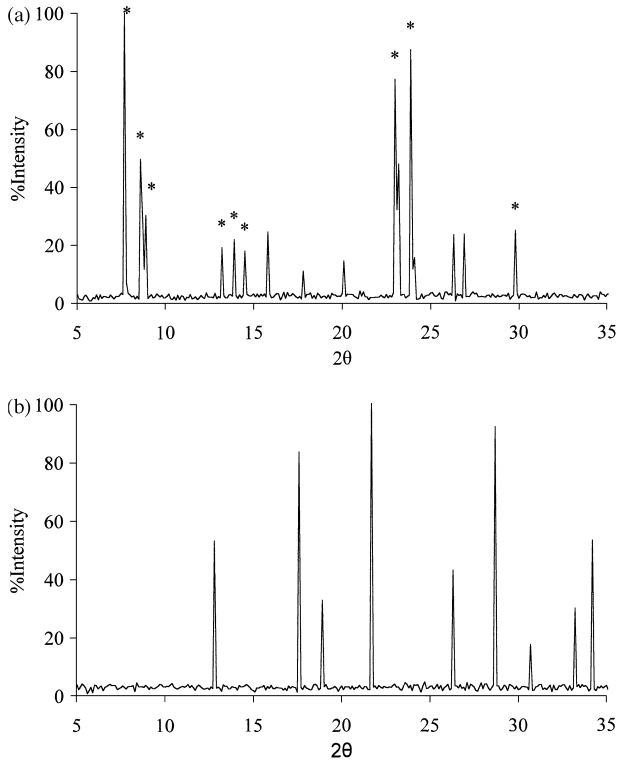

Fig. 1. (a) XRD pattern of the silicalite layer synthesized on top of the macroporous substrate (asterisks denote silicalite peaks); (b) XRD pattern of the macroporous alumina substrate.

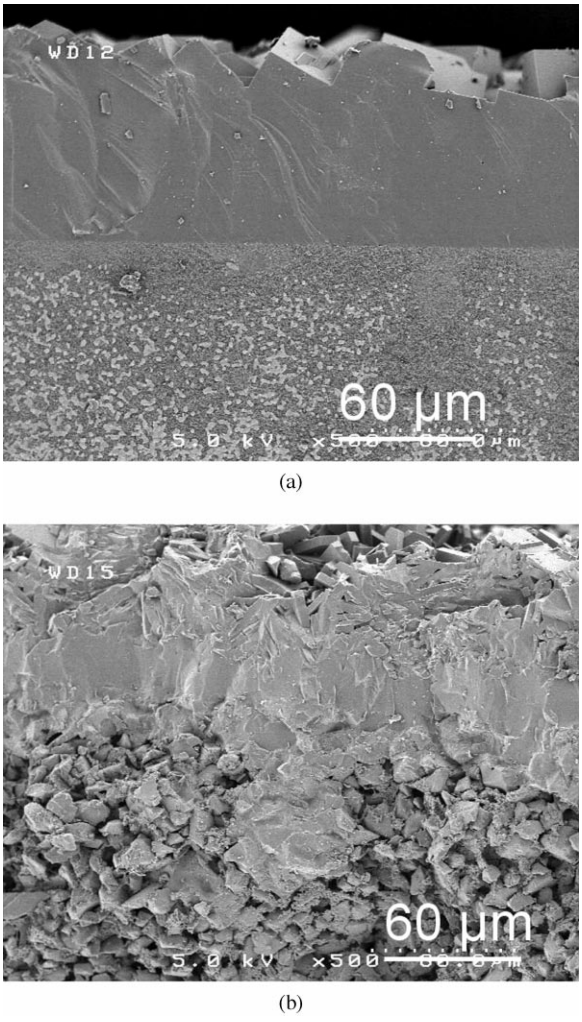

Fig. 2. SEM showing a cross-section of a silicalite-1 membrane on a porous α-Al_2O_3 substrate having a mean pore diameter of (a) 0.08 μm, (b) 9 μm.

Hg porosimetry provided a detailed insight into the mechanism of the growth of zeolite phase, in the macropore structure of the alumina support. Investigations were made using supports with the same pore sizes for different reaction conditions (time, temperature). Typical results of Hg porosimetry before (alumina substrate 0.15 μm — curve a) and after synthesis at two different temperatures and times (190°C for 1 day and 180°C for 3 days) are compared in Fig. 3. From curve b it is evident that cumulative intrusion volume for the sample with silicalite grown for 3 days at 180°C, stays constant above the threshold diameter of 0.15 μm and is reduced by a volume of 0.05 ml/g (from 0.18 to 0.13 ml/g) below that point. This gives some strong indication that the zeolite phase has grown inside the macropores of the substrate. On the other hand, if one increases temperature and decreases the reaction time, entirely different results are obtained. It appears that for the sample with silicalite grown in it for 1 day at a temperature of 190°C (curve c), the cumulative intrusion volume is higher by a constant amount of around 0.05 ml/g both before and after the threshold diameter of 0.15 μm. This amount most likely corresponds to a thick zeolite layer formed on the outer surface of the alumina substrate and is also confirmed from SEM micrographs. The synthesis was repeated using the 0.08 μm alumina support. The reaction temperature for this sample was kept at 150°C but the reaction time was only 1 day. Under these conditions it was again possible to grow zeolite crystals mainly inside the much smaller, compared to the previous cases, macropores of the substrate. Thus it appears that higher temperatures lead to rapid nucleation and zeolite crystal growth, resulting to the formation of thick layers formed on the outer surface of the substrate. On the other hand, lower temperatures lead to a more amorphous and disordered zeolite phase, which is mainly located inside the macropores of the substrate. The higher synthesis temperature for silicalite-1 may also result in an attack of the surface of the support and give rise to an anchoring of zeolite.

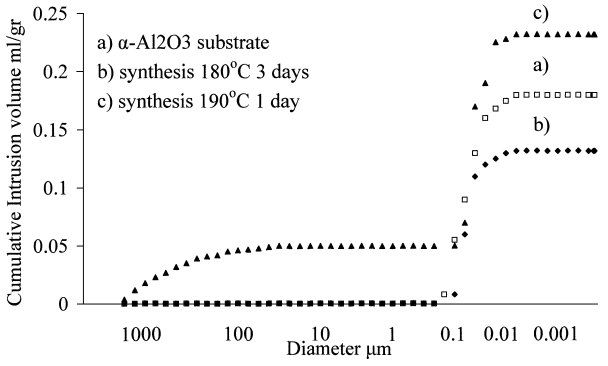

Fig. 3. Hg intrusion–extrusion data porosimetry before (α-Al_2O_3 substrate 0.15 μm — curve a) and after synthesis at 180°C for 3 days (curve b) and 190°C for 1 day (curve c).

Nitrogen porosimetry enables one to get information regarding the types of micro- or mesopores that exist in a porous material by constructing the corresponding nitrogen adsorption/desorption isotherm. In Fig. 4, nitrogen porosimetry results are shown for the grown silicalite. The shape of the isotherm is type II, which is typical of microporous materials. The surface area and the micropore volume of the sample were calculated using the DR (Dubinin-Radushkevich) approximation and found to be 454.75 m^2/g and 0.16 cm^3/g.

On the other hand, part of the substrate (from the silicalite side) was scratched away and analyzed with nitrogen sorption at 77 K (Fig. 5, curve a). In this case, the isotherm is type IV (mesoporous) including microporosity (a sharp increase of the isotherm is observed at low relative pressures (Fig. 5, inset), which indicates the presence of silicalite inside the alumina structure, while the N_2 for the untreated substrate shows a typical non porous behaviour (Fig. 5, curve b).

3.3. Gas transport behaviour

Two of the developed membranes on supports of different porous size (0.08 and 0.15 μm), synthesised at the

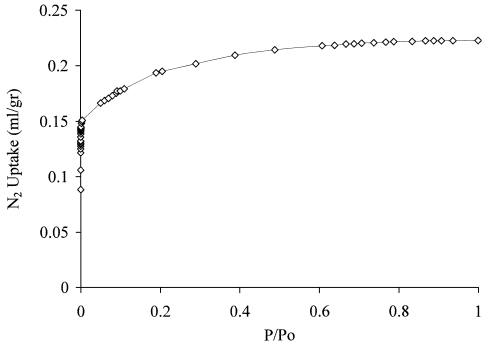

Fig. 4. N_2 adsorption isotherm at 77 K of the silicalite-1 layer scratched from the top of the composite membrane.

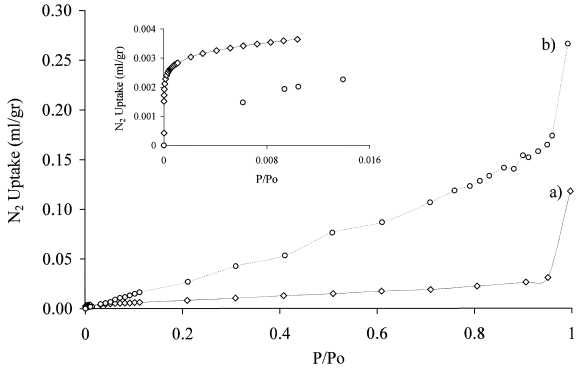

Fig. 5. N_2 adsorption isotherm at 77 K of the top section of the macroporous substrate (curve a) and for the untreated macroporous substrate (curve b). Inset: Low pressure data showing micropore behavior.

same hydrothemal conditions (180°C for 3 days), were examined by helium differential permeability experiments at 308 K and exhibited a typical crack (macropore) free behaviour. Knudsen regime is predominant when the radius, r, of the pore is much smaller than the mean free path, λ, of the permeating molecule ($r/\lambda \rightarrow 0$). As the mean pressure increases (λ decreases), the flow regime changes from Knudsen (permeance independent of the mean pressure, p_{mean}) to Poisseuille (permeance proportional to p_{mean}), as pointed out in Fig. 6(a). From this figure it is clear that this change from molecular to viscous flow, for both membranes, occurs at approximately 12 bar, where the mean free path of helium for the aforementioned temperature is 168 Å. By making the usual assumption that Knudsen regime changes to viscous when $0.01 < r/\lambda < 0.05$,[17] one can calculate that the pore diameters range between 3.4 and 16.9 Å, excluding thus the existence of macro and mesopore intercrystalline voids. Furthermore, when macropores (cracks) are present, the flow is expected to be Poisseuille even at very low pressures, as presented in Fig. 6(b), which contains the differential permeance results for a membrane developed on a support of 9 μm porous size, and under different hydrothermal conditions (190°C for 1 day).

The temperature dependence of the integral permeance of helium was not Knudsen ($Pe \propto T^{1/2}$). The process was found to be activated and activation energies were derived assuming an Arrhenius type of behaviour via equation:

$$Pe = Pe_{\infty} e^{-E_a RT}$$

where Pe is the permeance, E the activation energy, T the temperature, Pe_{∞} the permeance at $T \rightarrow \infty$ and R the gas constant. The activation energy is then easily calculated from the slope of the lnPe vs. $1/T$ curve (Fig. 7). Although the permeability values are different, E_a is 6 kJ/mol for both membranes (Fig. 7, curves a and b). This is another strong indication that the porous network developed is the same in the two substrates (in terms of pore size, connectivity, constrictions, etc.), and this can only happen if transport occurs only through the zeolite phase.

The aforementioned membranes were furthermore analysed by single gas adsorption and permeability measurements. The membrane structure is formed by highly inter-grown and disordered crystal arrangements and hence the mass transport is much more complex and difficult to describe compared to single crystals. In Fig. 8(a) and (b) permeability data for several gases (He, N_2, CO_2, O_2, CH_4, C_2H_6, C_3H_8) are plotted against the feed pressure at 383 K for the two membranes with substrates of 0.08 and 0.15 μm, respectively. The ratio of the permeances of each gas for the two membranes gives a value of approximately 1.7, which is the exact ratio of the volume loss of the substrates (obtained from Hg porosimetry results). By carrying out simple calculations it can be proved that the growth of silicalite-1 crystals inside the pores is defect free. It is well known that the permeance is calculated by the following equation:

$$Pe = \frac{J}{U \Delta P}$$

where J is the flux (mol/s), U the area of the membrane in m^2 and ΔP the pressure difference across the membrane in kPa. By dividing the permeances of the two membranes (different supports) the following equation holds:

$$\frac{Pe_{0.15}}{Pe_{0.08}} = \frac{U^{sil}_{0.15}}{U^{sil}_{0.08}} = \frac{U^{sil}_{0.15} \times \ell}{U^{sil}_{0.08} \times \ell} = \frac{V_{0.15}}{V_{0.08}}$$

where U^{sil}_i is the cross-sectional area of silicalite-1 grown in the pores of substrate i, ℓ the thickness of the zeolite layer in and V_i the apparent volume of zeolite phase (obtained from differences in total pore volume before and after synthesis). Assuming the same penetration depth of the zeolite phase into the macropores (same synthesis conditions) of the two substrates, the permeances measured should be proportional to the zeolite volume, if all macropores are blocked by zeolite, as it seems to be.

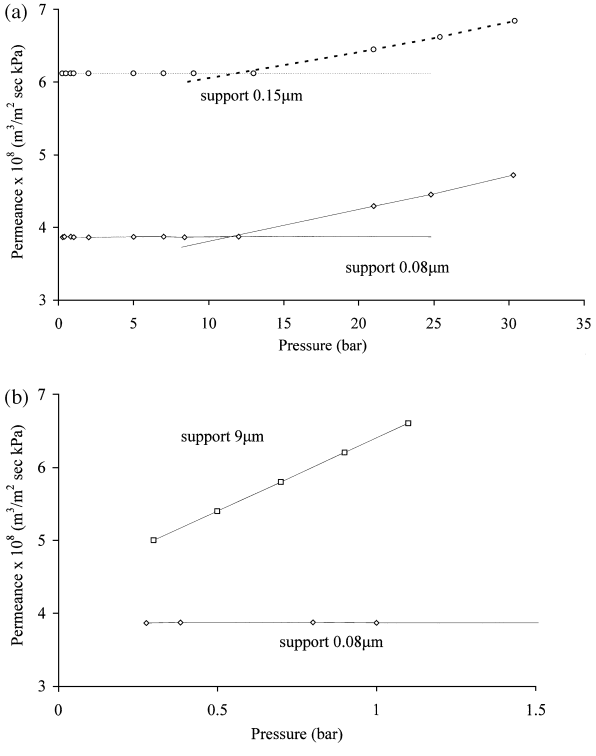

Fig. 6. He differential permeances at 308 K of the composite membranes: (a) α-Al_2O_3 substrate 0.08 μm and α-Al_2O_3 substrate 0.15 μm; (b) α-Al_2O_3 substrate 9 μm.

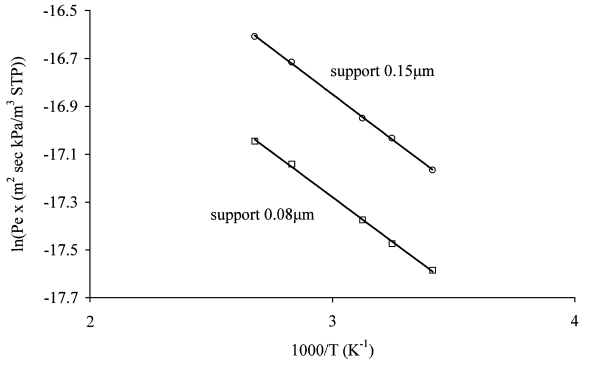

Fig. 7. Calculation of activation energy for helium.

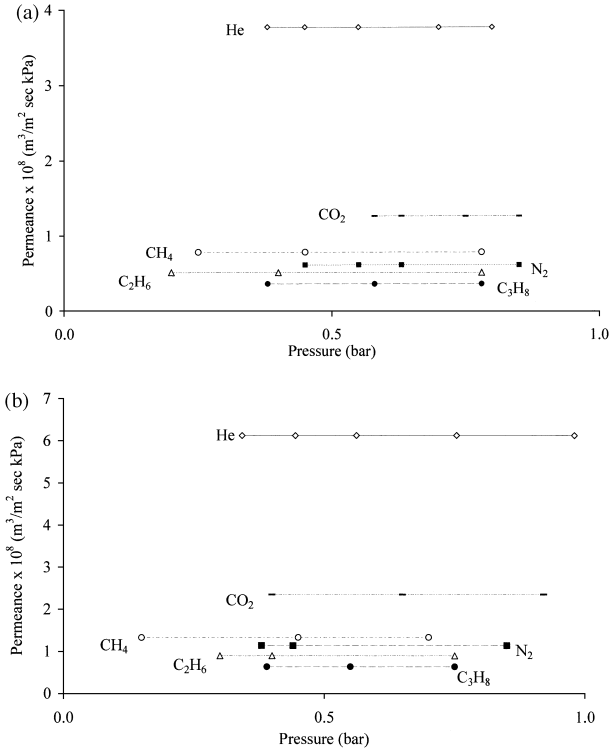

Fig. 8. Permeances of several gases at 383 K as a function of the feed pressure: (a) α-Al_2O_3 substrate 0.08 μm and (b) α-Al_2O_3 substrate 0.15 μm.

Additionally SF_6 was used as a probe molecule and the experiments were performed via the Wilke–Kallenbach method. Nitrogen was used as sweep gas, flowing on the substrate side. The zeolite side was fed with a mixture of helium and SF6. Both sides were kept at atmospheric pressure. The lowest calculable permeance value, limited by the analytical ability of the thermal conductivity (TCD) detector, at the specific setup, is 1.4×10^{-14} (m^3/m^2 s kPa). Under the above conditions, no flux of SF6 was detected or else, its permeance was lower than the aforementioned limit.

The influence of the orientation of the zeolite layer as well as of magnitude of the fluxes at the feed and permeate sides, on the permeance of helium at 383 K were examined. The experiments were performed using the Wicke–Kallenbach method, with either carbon dioxide or nitrogen as sweep gases while the membrane (0.08 μm, substrate) was kept at atmospheric pressure on both sides. Results are summarized in Table 1. It is obvious that the permeance increases by a factor of approximately 2.3 when helium is introduced on the support side and nitrogen on the zeolite layer, but this factor falls to 1.1 using carbon dioxide as sweep gas. The increase of the permeance value is attributed to the fact that helium is more effectively removed from the permeate side, thus increasing the effective concentration gradient across the zeolitic layer. In the case of CO_2 the effect of enhanced concentration gradient is counterbalanced by the increased concentration of CO_2 molecules in the zeolitic pores (adsorption of CO_2), introducing thus an additive resistance to the helium flux, which is also observed by the lower values of helium permeances (Table 1). The augmentation of the fluxes in both sides had as effect higher permeance values, as a result of the lower concentration of the permeate substance at the permeate side, leading thus to a higher concentration gradient. The variation of the permeance values as a function of the flux was almost identical for both orientations of the membrane, and exhibited an increase by a factor of 1.5 when the flux was three times higher.

Furthermore the quality of the produced membrane and the defect (macropore) free growth of the zeolite layer were certified via CO_2/He permeability experiments at elevated pressures. The experiment was performed at 308 K, and the membrane was fed with 10 ml/min He on the support side, while 10 ml/min carbon dioxide were flowing past the zeolite layer. The steady state helium permeances were measured for all the successive increments of pressure (both sides) from 1 to 10 bars. No helium was detected at the zeolite layer side when the pressure reached the value of 8 bars, which corresponds to the complete filling of pores, as indicated by the carbon dioxide Isotherm at 308 K (Fig. 9).

3.4. Selectivity measurements

Selectivity measurments were performed with a mixture of *n*-hexane, 2,2-dimethylbutane. Both molecules have high adsorption potential at low temperatures (measured values of the Langmuir constant are 9.85×10^{-4} and 2.15×10^{-4} Pa^{-1} at 443 K, respectively). It is evident that the external surface of the zeolite will be occupied in a large extent by both molecules, as experiments were performed at high feed pressures, well above the Henry region. On the other hand the smaller *n*-hexane molecule which can easily enter the zeolite pore will have a high occupation degree compared with the 2,2-dimethylbutane which can hardly enter the zeo-

Table 1
Effects of the orientation of the membrane, of the flow rate at the permeate side and of the sweep gas, on helium permeance at 373 K

Seep gas	Orientation	Flow rate (ml/min)	Permeance (m^3/m^2 s kPa)
Nitrogen	From zeolite to support	10	5.339E-09
		20	6.633E-09
		30	7.604E-09
	From support to zeolite	10	1.124E-08
		20	1.580E-08
		30	1.628E-08
Carbon Dioxide	From zeolite to support	10	3.370E-09
	From support to zeolite	10	3.552E-09

Table 2
Selectivity of *n*-hexane/2,2,DMP on a silicalite membrane

T (K)	Feed (kPa/kPa) (*n*-hexane/2,2,DMB)	Flow rate at the permeate side (ml/min)	Mixture selectivity (*n*-hexane/2,2,DMP)
373	1.17	15 20 25	18.9 22.1 27
	0.65	15 20 25	18 20 22.4
	0.25	15 20 25	13 15.7 18
	2.32	15 20 25	23 26 30
323	1.2	15 20 25	23.5 25 29
	0.85	10 20 25	18.2 24 26
	1.6	10 20 25	21.4 26.3 32.5
308	1.03	10 20	24 27.4
	1.36	20 25	28 29

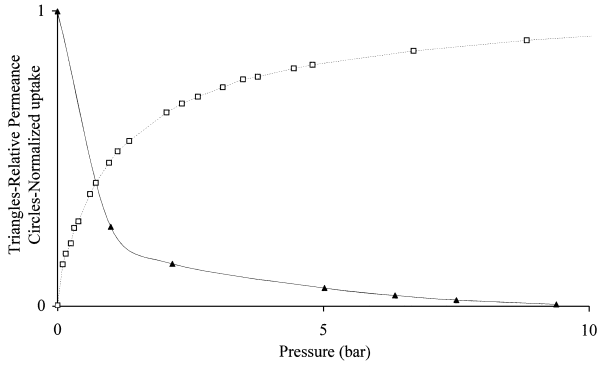

Fig. 9. Carbon dioxide isotherm on silicalite-1 at 308 K (normalized uptake values) and relative permeance of helium as a function of the pressure for a CO_2/He experiment at 308 K.

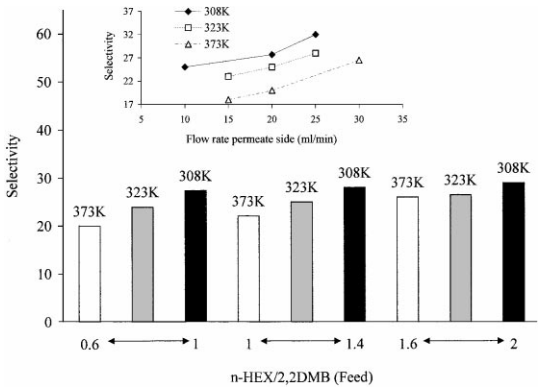

Fig. 10. Histogram showing the *n*-HEX/2,2DMB selectivity capacity of the silicalite-1 membrane (substrate 0.15 μm), as a function of the temperature and the feed *n*-HEX/2,2DMB ratio (kPa/kPa). Inset: Effect of the flow rate at the feed side and temperature on the selectivity capacity of the membrane.

litic pores. As a result, the intracrystalline diffusion of *n*-hexane will not be influenced by the presence of the branched molecules. It is obvious that a change of the concentration of the mixture at the feed side in favour of the larger 2,2-dimethylbutane molecules, increases the posssibility of the blocking of the pore apperture for the *n*-hexane molecules which will effect the direct entrance of *n*-hexane from the gas phase and as a result the separation capacity of the membrane will be reduced. Preliminary selectivity results are shown in Table 2 and illustrated in Fig. 10. As can be seen from the above results, a selectivity between 16 and 30 is obtained by varying the temperature from ambient conditions and up to 100°C. It is important to observe that an increase in temperature results in a dramatic decrease in the mixture selectivity. This is because the branched paraffin (2,2,DMB) is activated at high temperatures resulting in higher permeation rates and thus in a decrease in selectivity of *n*-hexane over 2,2,DMB. It is expected that at even higher temperatures (around 180–200°C) the selectivity will drop to a value of around 1 making the zeolite membrane incapable of separating the aforementioned gas mixture. Thus the temperature region one should work at, in order to achieve a sufficient degree of separation for the mixture *n*-hexane/2,2, DMB should not exceed 100–120°C. Lower temperatures will favour separation while higher temperatures will have the opposite effect.

Another point that should be mentioned and which is indicative of the absence of mesopores, is that during the selectivity experiments, neither nitrogen or helium (feed and sweep gas respectively) were detected at the feed and permeate side of the membrane. The relative pressures (P/P_o) of both organic liquids in the feed stream, for the aforementioned temperatures were very low (between 0.1 and 0.2 at 308 K, 0.07 and 0.13 at 323 K and 0.015 and 0.03 at 373 K) to bring on blocking of mesopores, if were present.

4. Conclusions

The synthesis and characterisation of silicalite-1 membranes on porous alumina ceramic supports have been described here. It has been shown that by controlling the

synthesis conditions it is possible to optimise the growth and structure of silicalite-1 membranes. At lower synthesis temperatures (150°C), the growth of silicalite inside the macro-pore of the ceramic support is favoured, while at higher temperatures (190°C), thick, well-crystallised zeolite layers develop from the surface of the support. A more stable membrane is obtained if the zeolite phase is formed predominantly inside the pores of the support. Furthermore, the zeolite layer structure and the penetration depth depend on the type of macro-porous support used for the synthesis. A more homogenous silicalite-1 film, together with a lower degree of penetration, was obtained for the alumina support having the smaller macropores (0.08 μm) compared to the more rugged film on the surface of the support having larger pores (9 μm) as indicated by SEM micrographs. To obtain defect free membranes it is again preferable to have zeolite growth inside the support sub layer. To achieve this, a control of the formation of the gel phase, which precedes the nucleation of the zeolite, is necessary.

The quality of two membranes was checked by a variety of methods such as XRD, SEM, Hg porosimetry and low-pressure integral permeability for various gases at different temperatures. SF6 was not permeating and the ratio of permeabilities of the two samples, for all the gases used, corresponds to the ratio of the zeolite volumes, as expected for defect free membranes. On the other hand the same activation energies for transport have been calculated for both samples and since the activated behaviour is attributed to hindered diffusion of molecules in the zeolite pores, we have a strong indication that mass transfer is controlled only by the zeolite phase. Furthermore, the production of defect free membranes was certified via a complete set of permeation experiments including high-pressure, differential (He) and counter-current (He/CO_2) experiments. High-pressure experiments revealed a change in the flow regime (Knudsen to Poisseuille) at a pressure of approximately 12 bar, indicating the absence of defects even in the mesopore range. In the He/CO_2 experiment, cut off of helium permeation was observed at a pressure of 8 bar, corresponding to the complete filling of micropores by CO_2, as calculated from the adsorption isotherm. Additionally, the influence of membrane's orientation as well as feed and sweep gas flow rates on the permeability was examined. Finally, *n*-HEX/2,2 DMB selectivity measurements were performed and a selectivity of about 30 was calculated. Large separation factors for gas mixtures, which are currently under investigation, are expected to be achieved with these membranes.

Acknowledgements

We are indebted to Dr. Velterop and Mr. Weierink for kindly providing the ceramic supports. This work was funded by the European Community under the Industrial and Materials Technologies Programme (Brite-Euram III; Contract No. BRPR- CT96- 313).

References

1. Bhave, R. R., *Inorganic Membranes, Synthesis, Characteristics and Applications*. Van Nostrand Rheinhold, New York, 1991.
2. Larbot, A., Fabre, J. P., Guizard, C. and Cot, L., *J. Membrane Sci.*, 1988, **39**, 203.
3. Larbot, A., Fabre, J. P., Guizard, C., Cot, L. and Gilot, G., *J. Am. Ceram. Soc.*, 1989, **72**, 257.
4. Jansen, J. C., Kashiev, D. and Erdem-Senatalar, A., Preparation of coatings of molecular sieve crystals for catalysis and separation. In *Advanced Zeolite Science and Applications. Stud. Surf. Sci. Catal. 85*, ed. J. C. Jansen, M. Stöcker, H. G. Karge and J. Weitkamp. Elsevier, Amsterdam, 1994, pp. 215–250.
5. Uzio, D., Peureux, J., Giroir-Fendler, A., Dalmon, J. A. and Ramsay, J. D. F., Formation and pore structure of zeolite membranes. In *Characterization of Porous Solids III. Stud. Surf. Sci. Catal. 87*, ed. J. Rouquerol, F. Rodriguez-Reinoso, K. S. W. Sing and K. K. Unger. Elsevier, Amsterdam, 1994, pp. 411–418.
6. Barrer, R. M., *Hydrothermal Chemistry of Zeolites*. Academic Press, London, 1982.
7. Moscou, L., The zeolite scene. In *Introduction to Zeolite Science and Practice. Stud. Surf. Sci. Catal. 58*, ed. H. van Bekkum, E. M. Flanigen and J. C. Jansen. Elsevier, Amsterdam, 1991, pp. 1–12.
8. Yan, Y., Davis, M. E. and Gavalas, G. R., Preparation of zeolite ZSM-5 membranes by in-situ crystallization on porous α-Al_2O_3. *Ind. Eng. Chem. Res.*, 1995, **34**, 1652–1661.
9. Minot, S., Headland, J., Schulman, B., Valtchev, V. and Sterte, J., Continuous films of zeolite ZSM-5 on modified gold surfaces. *Chem. Common.*, 1997, 15–16.
10. van Bekkum, H., Guess, E. R. and Kouwenhoven, H. W., Supported zeolite systems and applications. In *Advanced Zeolite Science and Applications. Stud. Surf. Sci. Catal. 85*, ed. J. C. Jansen, M. Karge, H. G. Karge and J. Weitkamp. Elsevier, Amsterdam, 1994, pp. 509–542.
11. Jia, M. D., Chen, B., Noble, R. D. and Falconer, J. L., Ceramic-zeolite composite membranes and their application for separation of vapour/gas mixtures. *J. Membrane Sci.*, 1994, **90**, 1–10.
12. Baker, W. J. W., Kapteijn, F., Poppe, J. and Moulijn, J. A., Permeation characteristics of a metal supported silicalite-1 zeolite membrane. *J. Membrane Sci.*, 1996, **117**, 57–78.
13. Baker, W. J. W., Van den Broeke, L. J. P., Kapteijn, F. and Moulijn, J. A., Temperature dependence of one-component permeation through a silicalite-1 membrane. *Aichi. J.*, 1997, **43**, 2203–2214.
14. Van de Graaf, J. M., Van deer Bill, E., Stool, A., Kapteijn, F. and Moulijn, J. A., Effect of operating conditions and membrane quality on the separation performance of composite silicalite-1 membranes. *Ind. Eng. Chem. Res.*, 1998, **37**, 4071–4083.
15. Van de Graaf, J. M., Kapteijn, F. and Moulijn, J. A., Methodological and operational aspects of permeation measurement on silicalite-1 membranes. *J. Membrane Sci.*, 1998, **144**, 87–104.
16. Steriotis, T. A., Katsaros, F. K., Mitropoulos, A.Ch., Stubos, A. K., Galiatsatou, P., Zouridakis, N. and Kanellopoulos, N. K., Novel design for high pressure, integral, differential, absolute, and relative multicomponent permeability measurements. *Review of Scientific Instruments*, 1996, **77**, 2545–2548.
17. Kainourgiakis, M. E., Stubos, A. K., Konstantinou, N. D., Kanellopoulos, N. K. and Milisic, V., A Network model for the permeability of condensable vapours through mesoporous media. *J. Membrane Sci.*, 1996, **114**, 215–255.